

LED-backlight feedback control system with integrated amorphous-silicon color sensor on an LCD panel

Ki-Chan Lee
Seung-Hwan Moon
Brian Berkeley
Sang-Soo Kim

Abstract — Thin-film-transistor liquid-crystal displays (TFT-LCDs) have the largest market share of all digital flat-panel displays. An LCD backlighting system employing a three-color red-green-blue light-emitting diode (RGB-LED) array is very attractive, considering its wide color gamut, tunable white point, high dimming ratio, long lifetime, and environmental compatibility. But the high-intensity LED has problems with thermal stability and degradation of brightness over time. Color and white luminance levels are not stable over a wide range of temperature due to inherent long-term aging characteristics. In order to minimize color point and brightness differences over time, optical feedback control is the key technology for any LED-backlight system. In this paper, the feasibility of an optical color-sensing feedback system for an LED backlight by integrating the amorphous-silicon (a-Si) color sensor onto the LCD panel will be presented. To minimize the photoconductivity degradation of a-Si, a new laser exposure treatment has been applied. The integrated color-sensor optical-feedback-controlled LED-backlight system minimized the color variation to less than $0.008 \Delta u'v'$ (CIE1976) compared to 0.025 for an open-loop system over the temperature range of 42–76°C.

Keywords — Color sensor, integrated sensor, amorphous silicon, LED backlight, TFT-LCD, photo-stability, dangling bond, photoconductor, feedback.

1 Introduction

LCDs with LED backlights are obvious candidates for flat-panel displays used in TV applications. The color reproduction of LED-backlit LCDs easily surpasses that of PDPs or CRTs. The red, green, and blue (RGB) LED backlight can provide almost any visible color in a compact form factor, and it offers unique features such as instant color adjustment.^{1,2} LED backlights are very attractive considering their wide color gamut, tunable white point, high dimming

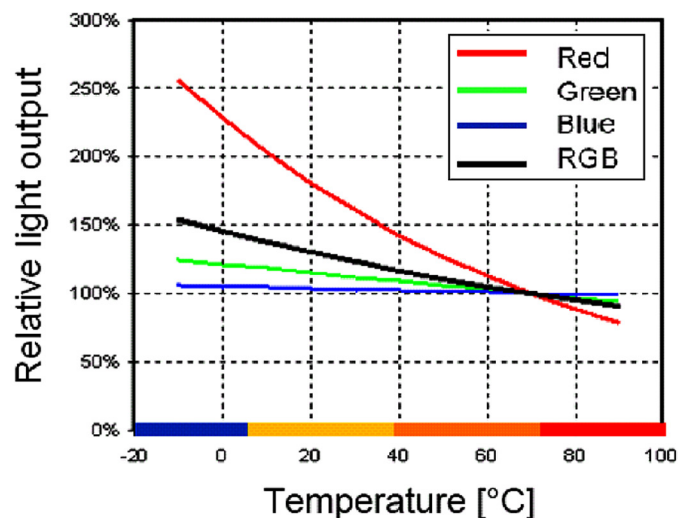


FIGURE 1 — Relative light output of RGB-LEDs as a function of substrate temperature.

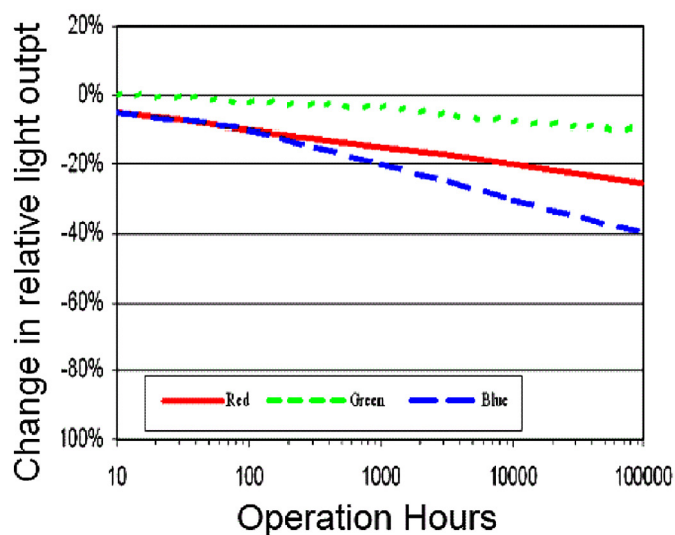


FIGURE 2 — Change in relative light output of RGB LEDs as a function of operating time.

ratio, long lifetime, and environmental compatibility. Furthermore, LED-backlit LCDs offer potential application for high dynamic contrast ratio by way of localized backlight driving, motion-picture-quality improvement by means of backlight blinking, and cost reduction using color-filter-less field-sequential display technologies.

However, compared to cold-cathode fluorescent lamps (CCFLs), the high intensity LED has relatively lower efficacy and has problems with thermal and aging stability.³ Therefore, LED-backlight color point and white luminance

Extended version of a paper presented at the 2005 SID International Symposium held May 24–27, 2005, in Boston, Massachusetts.

The authors are with Samsung Electronics, Technology Development Group, LCD Development Center, LCD Business, Myeongam-ri 200, Asan-si, Chungnam-do 336-841, Korea; telephone +82-41-535-3087, fax -1097, e-mail: kc77.lee@samsung.com.

© Copyright 2006 Society for Information Display 1071-0922/06/1402-0161\$1.00

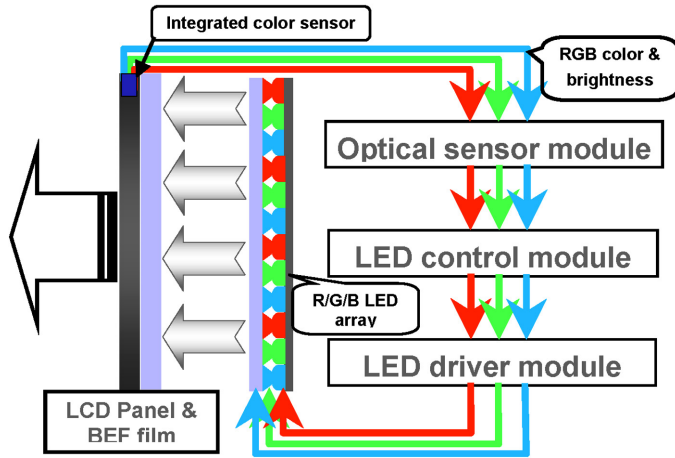


FIGURE 3 — LED-backlight system with optical feedback control.

levels are not stable over a wide range of temperature or operating life due to the inherent characteristics of the LEDs.

2 Optical-feedback requirement

Figures 1 and 2 depict the relative instability of the red, green, and blue LED backlight sources. Figure 1 shows the relative light output for each of the LED sources as a function of the temperature of the substrate on which the LED chip is mounted. Change in relative light output of the RGB-LEDs with time is shown in Fig. 2. Without some means of closed-loop control, these variations would result in serious color point and brightness deviations over both temperature and time.

Therefore, in order to minimize color-point and brightness differences over temperature and time, optical feedback control is the key technique for any LED-backlight system. There are many practical issues in implementation such as placement of the photosensor, sampling of light signals for feedback, effect of the LED drive current waveform on sensor signal integrity (crosstalk), and control system design. A three-color RGB LED-backlight system with an integrated color sensor on the LCD panel is depicted in Fig. 3.

3 Sensor considerations

3.1 Sensor placement

To accurately detect color and luminance in large-sized (>40-in.) panels using LED backlights, at least two color sensors are required, one each for the upper and lower portions of the display. Measurement accuracy is affected by the degree to which the color sensor is tilted from its mounting pad during the assembly process. The best place to attach the color sensor is either at the corner or along the edge of the backlight module. Furthermore, the best place for measuring the mixed RGB light from the backlight source

would be on the LCD panel itself. However, it is difficult to attach an external sensor and its circuitry to the LCD glass in a position perfectly aligned over an aperture that would be made in the narrow black border around the edge of the panel. Moreover, doing so would increase production cost and process time. In our work, we have developed a new technology for measuring the color point and white luminance of the LED backlight by using an a-Si photoconductive sensor integrated onto the LCD panel.

3.2 Sensor selection

Amorphous-silicon possesses well known photosensitive properties.^{4,5} a-Si:H is an excellent material from the viewpoint of high photosensitivity in the visible-light region, short response time, thermal stability, low process temperature, and high production yield. We considered three candidates for an integrated panel sensor, namely, TFT, photodiode, and photoconductive sensors.

A TFT would seem like an obvious candidate for an integrated sensor. However, to prevent the photosensitive properties of the TFT from adversely affecting the switching characteristics of the LCD, nearly all LCD manufacturers are applying a bottom-gate topology. The bottom-gate metal covers the active region of α -Si:H, thereby blocking the TFT from the backlight illumination. Clearly in the case

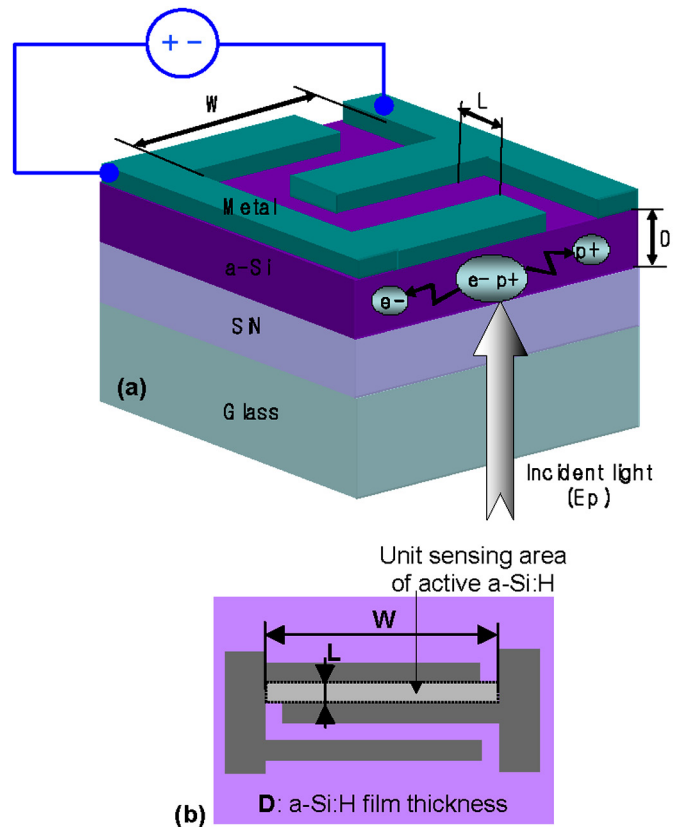


FIGURE 4 — (a) Photon-induced mobile-carrier generation of a-Si, (b) one segment of the sensor highlighted as $L \times W$.

of a sensor, the TFT would need to be illuminated. Also, available sensing area using a TFT would be small.

The most widely used optical sensor is a PN- or PIN-structured photodiode. The photodiode has fast response time and proven long-term stability; however, its low sensitivity and small sensing area are drawbacks. Moreover, fabrication of such a device as an integrated sensor would require P-doping, which would require an extra process step and would not be compatible with conventional TFT-LCD fabrication processes. The third option, the photoconductive optical sensor, has a very simple structure and is completely compatible with current TFT-LCD processes. The long minority carrier lifetime and high mobility of carriers inside the photoconductive sensor enables high dynamic range. The large passive area of a-Si provides high sensitivity. This structure offers benefits of simplicity, compactness, and sensitivity without the drawbacks of the other options. Therefore, we selected the photoconductive sensor for our system.

3.3 Sensor: Theoretical modeling

A physical model of the photoconductive sensor is shown in Fig. 4(a). The sensor works as a result of changes in photoconductivity at different light intensities. The generated electrons and holes from the incident photon energy move to the metal electrodes by the external electric field shown in Fig. 4(a). Carrier generation depends on the monochromatic photon flow rate N ($1/\text{cm}^2\text{-sec}$) which is related to the intensity I_L (W/cm^2) and photon energy $E_P (= h\nu, \text{W}\text{-sec})$ of incident light as shown in Eq. (1).⁶ The incident light energy determines the carrier density of the a-Si optical sensor. For simplification, we could treat electrons as photo-generated carriers. In Eq. (2), photoconductivity (σ) is derived from electron mobility (μ), the electron lifetime (τ), electronic charge (e) and the photon-energy transfer rate (δ). Finally, the photo resistance is shown in Eq. (3), expressed by the a-Si thickness (D), electrode distance (L), and width (W) of the sensor. Unit sensing area between the inter-comb-shaped electrodes is shown in Fig. 4(b). If we define the length, the width, and the thickness of the film, the surface resistance of the a-Si active area would be expressed by Eq. (3).

$$N = I_L/E_P, \quad (1)$$

$$\sigma = e\mu\tau\delta N, \quad (2)$$

$$R = L/\sigma WD. \quad (3)$$

Photo-induced dangling bonds (defects) means broken atomic bonds, resulting from absorbed photon energy in the a-Si. Generation of these dangling bonds comes from the inherently weak and unstable bonding state of a-Si. The dangling bonds can easily capture the photo induced mobile carrier, which decreases the conductivity and causes instability of the sensor.

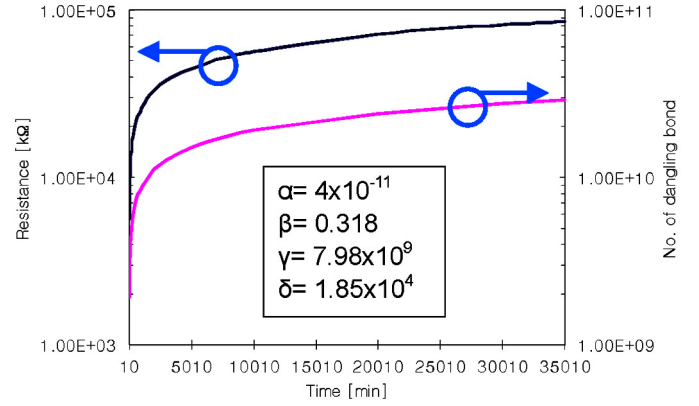


FIGURE 5 — Calculated number of dangling bonds and resistance of a-Si photoconductor.

In a-Si, the number of photo-induced dangling bonds (N_D) changes the conductivity, shown in Eq. (4) because the defect creation rate is proportional to the carrier recombination rate.⁷

The recombination process at the photo-induced defect is quite complicated because there are several possible transitions to steady-state conduction and valence energy levels. The photoconductivity in Eq. (4) is derived from the carrier mean free path (a_E), Boltzmann's constant (k), cross section for electron capture at defect (A), and temperature (T). In the photo-induced conduction state of a-Si, externally applied thermal energy interferes with the mobile carrier movement and decreases the conductivity.

To simplify, we define the Eq. (5), and the conductivity is given in Eq. (6). The generation rate of the dangling bonds is proportional to the illumination time and light intensity and defined in Eq. (7).⁷ Constant γ in Eq. (8) is the ratio of β to α extracted from the published literature.⁸ The resistance of the a-Si photoconductor is given as Eq. (9). Figure 5 shows the calculated number of dangling bonds and resistance of the a-Si photoconductor.

$$\sigma = \delta N e^2 a_E / 6 N_D A k T, \quad (4)$$

Let

$$\alpha = e^2 a_E / 6 A k T, \quad (5)$$

$$\sigma = \alpha \delta (I_L / N_D), \quad (6)$$

$$N_D(t) = \beta (\delta I_L)^{2/3} t^{1/3}, \quad (7)$$

Let

$$\gamma = \beta / \alpha, \quad (8)$$

$$R = \gamma (t / \delta I_L)^{1/3} (L / WD). \quad (9)$$

3.4 Panel-sensor integration

To minimize fabrication cost and increase the accuracy of the LED-backlight measurement, integration of the color sensor on the TFT-LCD panel is an attractive proposition. The a-Si photoconductive sensor with an RGB color filter

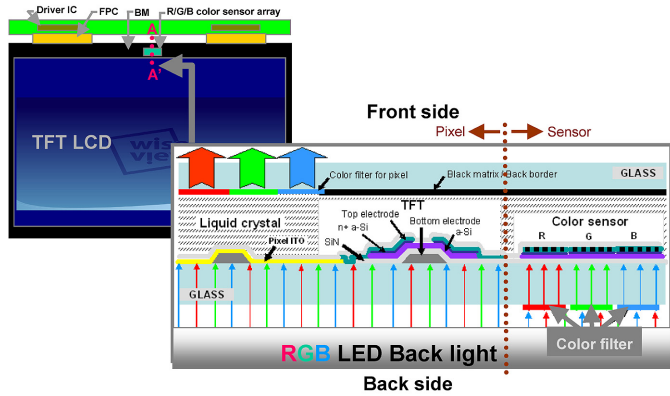


FIGURE 6 — a-Si photoconductive color-sensor integrated onto LCD panel.

was integrated on a 17-in. SXGA LCD panel as shown in Fig. 6. The color sensor is behind the black outer border of the LCD. The electrodes of the fabricated sensor in Fig. 7 have an inter-comb structure to maximize the photo-detection area and electron-drift channel width. The sensor electrode gap is $10\ \mu\text{m}$ with a channel width of $9000\ \mu\text{m}$ and total area of $1 \times 3\ \text{mm}^2$.

4 Laser stabilization of photosensor

The theoretical and experimental photo-resistance shown in Fig. 8 is inversely proportional to the incident-light intensity, mobility of the charge carrier, lifetime of the charge carrier, and photon-energy transfer rate. The problem reported on a-Si used as a photo-sensor is the change in photoconductivity due to long-term exposure to light.⁶ The change in resistance in the a-Si photoconductive sensor amounts to a $5\times$ increase compared to the original state after an exposure time of 2000 min as shown in Fig. 9. Many researchers started applying $\alpha\text{-Si:H}$ technology to image-sensing applications as early as 20 years ago, but the unstable response and low energy-transfer efficiency due to photo-induced defects impeded further investigation.^{9,10}

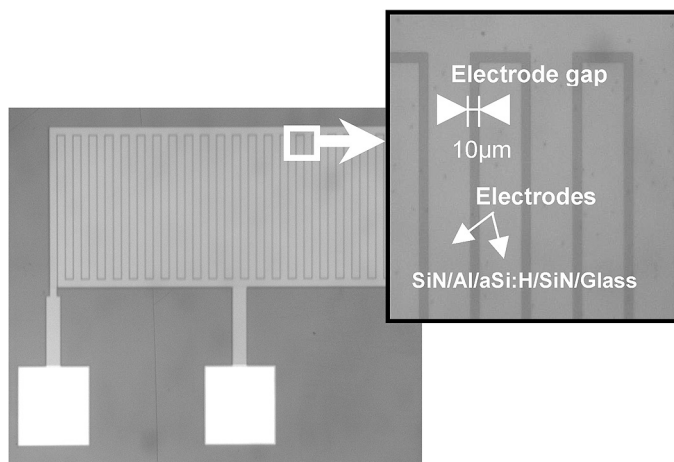


FIGURE 7 — Photograph of integrated $\alpha\text{-Si:H}$ photoconductive sensor fabricated by LCD process.

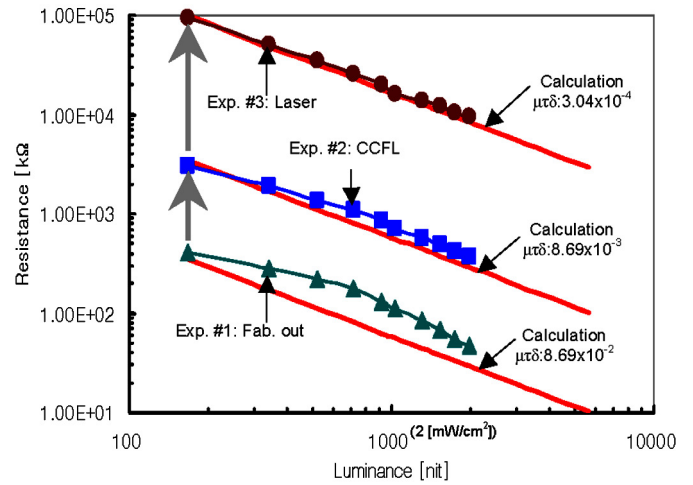


FIGURE 8 — Theoretical analysis and experimental results of photoconductivity at various light intensities.

We have developed a new approach for improving long-term photo-stability using high-energy-laser exposure. The instant high-energy light exposure process causes the $\alpha\text{-Si:H}$ to reach a saturated state of photo-induced dangling bonds. This photo-induced dangling bond saturation effect is equivalent to moving the sensor's photoconductivity to the flat portion (to the right) of the resistance curve shown in Fig. 5.

The characteristics of a-Si photo-stability after laser treatment are shown in Fig. 10(a). The a-Si has been treated with three different levels of laser energy. In the case of the 360-mJ/cm^2 laser-exposed sample, minimal photosensitive degradation is seen over a period of 35,000 minutes. It is important to apply a just-sufficient amount of laser energy to adequately saturate the dangling bonds. The photo-induced defect can be controlled theoretically in Eq. (7) with the exposure time and intensity of light. The correlation between the experimental and theoretical results of defect generation over time, with different levels of laser energy, is shown

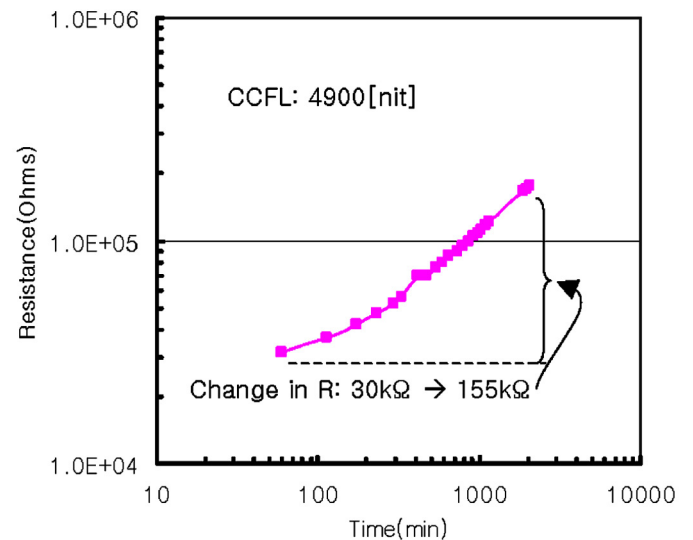


FIGURE 9 — Change in $\alpha\text{-Si:H}$ photoresistance due to light exposure.

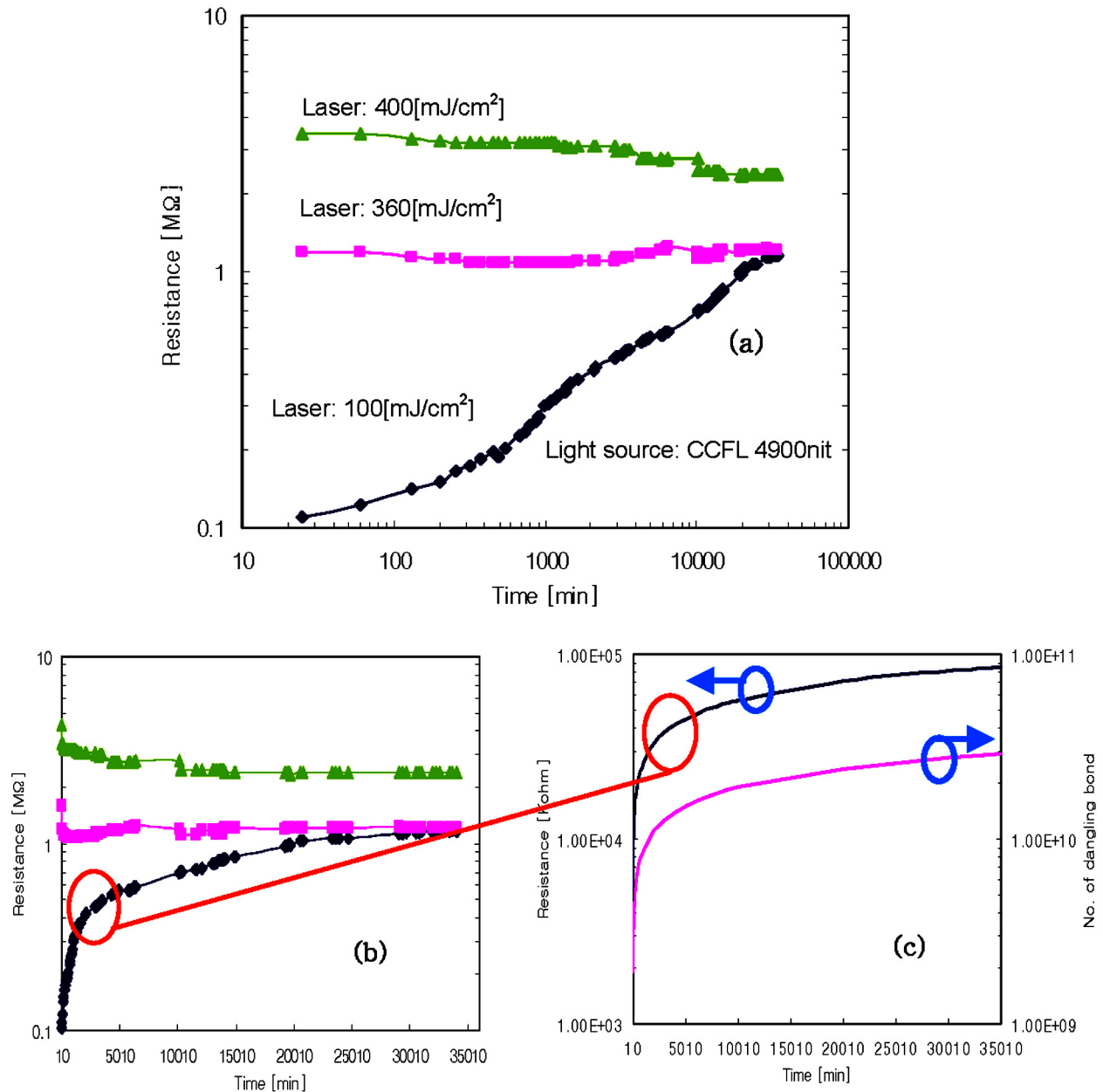


FIGURE 10 — (a) a-Si photo-stability change after exposure to different levels of laser energy, (b) analog scale of the experimental results, and (c) calculated result.

in Figs. 10(b) and 10(c). Figure 11 shows two sets of curves. All were taken from the same sensor. There are four curves taken before laser treatment and four taken after. At this state, the α -Si:H photo-sensor shows significant improvement in repeatability, about 98%, in comparison to 82% without the laser treatment.

5 Sensor performance

The readout circuit for the integrated sensor is implemented in a simple fashion with a half-bridge topology as shown in Fig. 12. The measured output waveform of the fabricated sensor versus a commercial photodiode sensor at the pulse signal input to the LED is shown in Fig. 13. Response

time is critical for accurate measurement of the pulse-width-modulated light output of the LED backlight. We compared the performance of our integrated photo-sensor with the commercial photodiode. The fabricated sensor has 100- μ sec faster response time compared to that of the commercial sensor. PWM driving input in Fig. 13 is applied to the LED for the measurement of response time. The a-Si:H photo sensor readout circuit is shown in Fig. 12, and the commercial photodiode was directly connected to the digital oscilloscope for detection of photovoltaic output.

Measured spectral sensitivity on the back and front sides of the optical sensor is shown in Fig. 14. The spectrum covers the entire visible range. To measure color, RGB color filters were placed at the back side of the fabricated optical

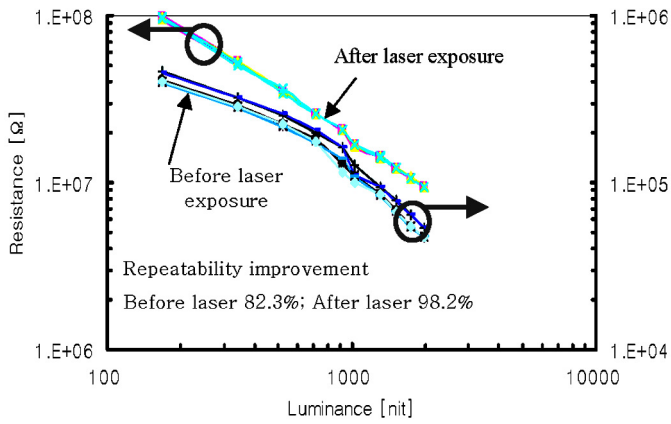


FIGURE 11 — Measured photo-stability and repeatability improvement after laser treatment of the fabricated optical sensor.

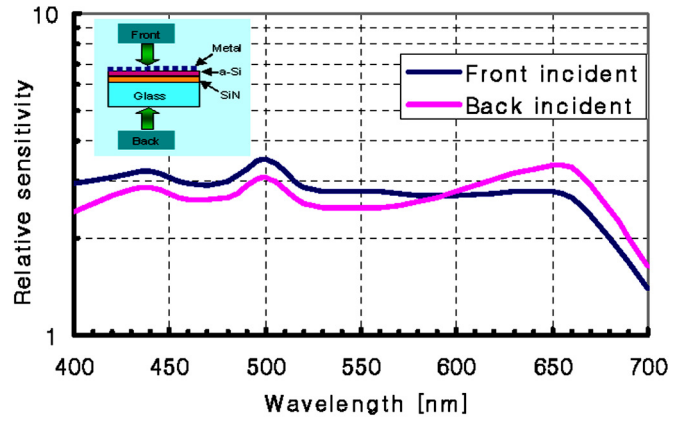


FIGURE 14 — Monochromatic spectral sensitivity of fabricated optical sensor.

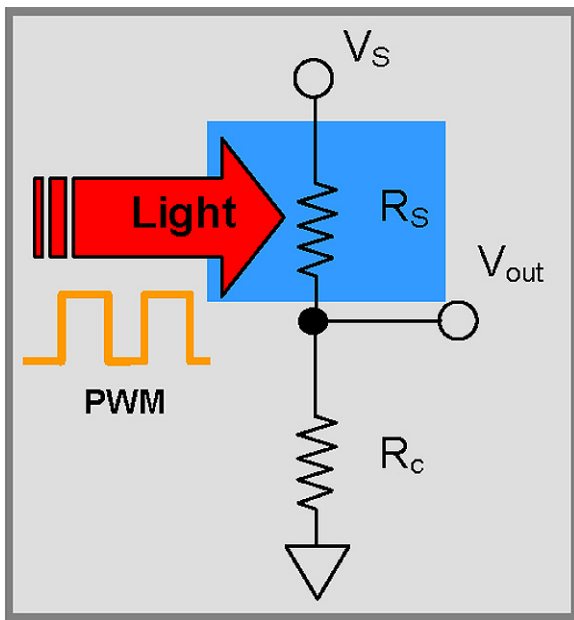


FIGURE 12 — Signal detection and driving circuit for the integrated sensor.

sensor. The energy transfer rate is a function of both photon quantum efficiency as well as material-absorption properties. The energy transfer rate δ of the sensor in Eq. (2) consists of the quantum efficiency and absorption rate of the photon energy. The quantum efficiency is the carrier-generation rate per incident photon. The absorption rate is the number of photons that reach the depth of the a-Si layer from the incident light.

The experimental result in Fig. 14 shows that high photon energy (short-wavelength region) does not always result in high sensitivity (low resistivity) in terms of a real device. This is due to the material properties, which have greater absorption at shorter wavelengths. The sensitivity of the sensor depends on the surface conductivity by the generated carrier density in the plane of the electrodes. Short-wavelength light generates more carriers due to high quantum efficiency. For this reason, sensitivity to front incident light is greater at the shorter wavelengths. However, the absorption rate of short wavelengths in a-Si film is reduced because short wavelengths can not penetrate deeply. For this reason, sensitivity to back incident light is greater at the longer wavelengths. Figure 15 shows the measured relative spectral sensitivity of the sensor with the color filter in place.

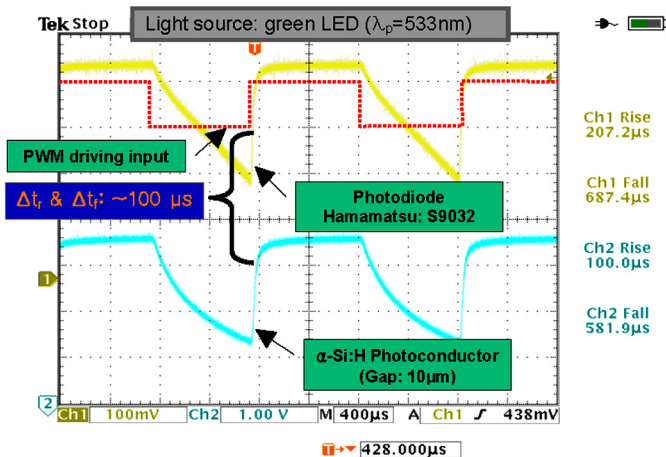


FIGURE 13 — Response-time comparison of integrated and commercial sensors.

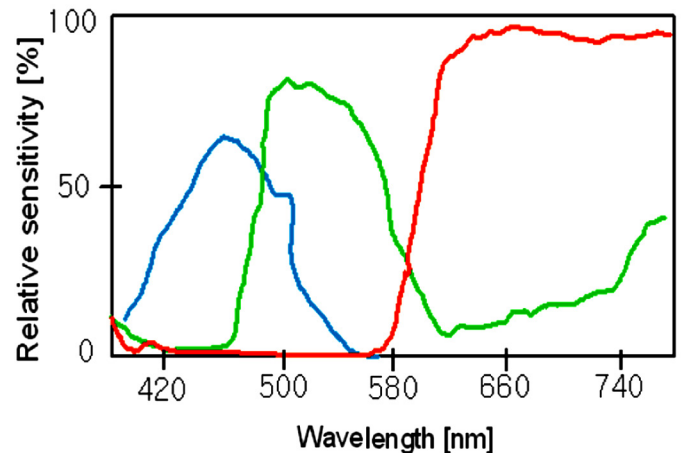


FIGURE 15 — Spectral sensitivity of the integrated sensor with color filter.

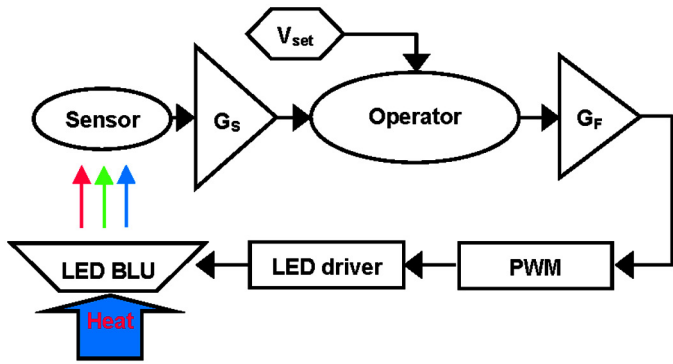


FIGURE 16 — Block diagram of optical feedback control system.

6 System design and results

The 17-in. LCD with an LED-backlight optical feedback control system utilizes the fabricated color sensor, signal-averaging amplification module (G_S), analog operation block, PWM generator, and feedback amplification (G_F) as shown in Fig. 16. In this system, the color sensor detects the luminance of each RGB LED and provides an electrical signal to the analog controller for comparison between initial set values (V_{set}) and the measured values. If there is a difference between the set and measured values, the controller compensates the PWM signal to the LED. The measured waveform of the averaged sensor output and PWM control signal for LED backlight feedback are shown in Fig. 17.

A comparison of color stability between the open loop and the optical-feedback closed-loop control systems is shown in Fig. 18. The optical-feedback-control LED-backlighting system with a color sensor integrated onto the LCD panel reduced the color variation ($\Delta u'v'$) to less than 0.008 compared to 0.025 for a non-feedback system. Additionally, white-luminance-level variation is controlled to be less than 5 nits.

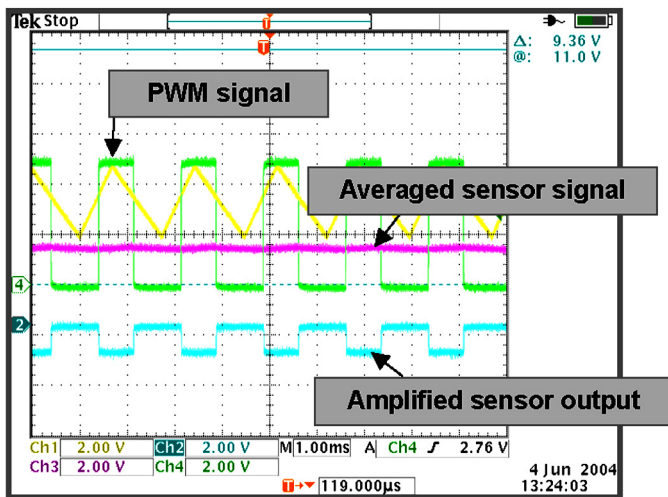


FIGURE 17 — Averaged sensor signal and PWM control-signal waveforms.

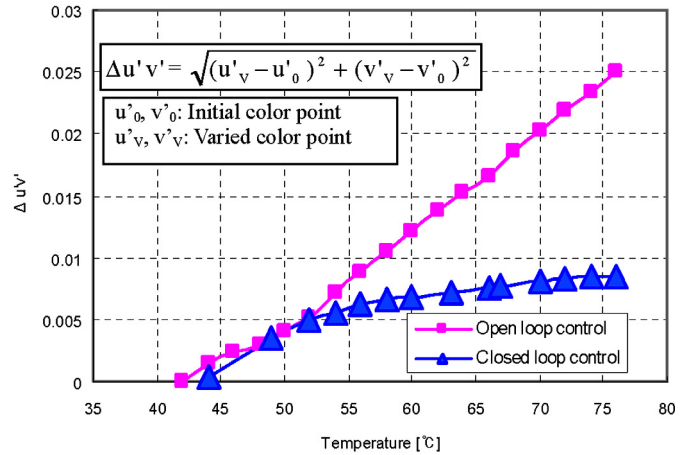


FIGURE 18 — Integrated-sensor closed-loop system performance improvement.

7 Conclusions

We have demonstrated the feasibility of an optical-feedback-controlled LED-backlighting system with an a-Si color sensor integrated onto the LCD panel. Integration of the color sensor provides a unique solution to the challenges posed by LED-backlight feedback systems including cost, photo-sensor placement, and sampling of light signals. The spectral sensitivity of the fabricated sensor without the color filter is nearly flat in response to both front and back incident monochromatic light sources. With the color filter in place, the integrated sensor shows suitable spectral sensitivity for detection of the RGB LED color and light intensity. Photo-degradation properties of a-Si were improved significantly with laser-exposure treatment. At this state, the α -Si:H photosensor shows significant improvement in repeatability, approximately 98%, in contrast to 82% without the laser treatment. The optical-feedback-controlled LED-backlighting system with integrated-on-panel color sensor improved the color variation ($\Delta u'v'$) to less than 0.008 compared to 0.025 for a non-feedback system. Additionally, white-luminance-level variation is controlled to be less than 5 nits over a temperature range of 42–76°C. For commercialization and mass production of the integrated color sensor on a TFT-LCD, temperature compensation of the sensor and a simpler embodiment of the color filter on glass will be developed in the future.

References

- 1 G Harbers and C G A Hoelen, "High performance LCD backlighting using high intensity red, green, and blue light emitting diodes," *SID Symposium Digest Tech Papers* **32**, 702–705 (2001).
- 2 S Muthu, F J Schuurmans, and M D Pashley, "Red, green, and blue LED based white light generation: Issues and Control," *IEEE J on Selected Topics in Quantum Electronics* **8**, 327–332 (2002).
- 3 Technical Presentation of Lumileds Lighting, LLC, <http://www.lumileds.com>.
- 4 D Horst, E Lueder, H Habibi, T Kallfass, and J Siegordener, "An array of TFT-addressed light sensors to detect grey shades and colors," *Sensors and Actuators A* **46**, 453–455 (1995).
- 5 D S Shen and H Ogura, "Integrated amorphous silicon photoconductive type image sensor," *Proc IEEE Southeastcon '92*, 358–362 (1992).

- 6 D L Staebler and C R Wronski, "Optically induced conductivity changes in discharge-produced hydrogenated amorphous silicon," *J Appl Phys* **51**, 3262–3268 (1980).
- 7 R A Street, *Hydrogenated Amorphous Silicons* (Cambridge University Press, 1991), pp. 213–320.
- 8 M Stutzmann, W B Jackson, and C C Tsai, "Kinetics of the Staebler–Wronski effect in hydrogenated amorphous silicon," *Appl Phys Lett* **45**, 1075–1077 (1984).
- 9 K Nakagawa, M Fukaya, T Shoji, K Sakai, and T Komatsu, "Stability and new structure in a-Si:H photoconductive sensors," *J Non-Cryst Solids* **59**, 1199–1202 (1983).
- 10 P J Zanzucchi, C R Wronski, and D E Carlson, "Optical and photoconductive properties of discharge produced amorphous silicon," *J Appl Phys* **48**, 5227–5236 (1977).



Ki-Chan Lee received his B.S., M.S., and Ph.D. degrees in electrical engineering from Kyungpook National University, Daegu Korea in 1992, 1998, and 2002, respectively. From Fall 2002 to Winter 2003, he worked as a post-doctoral research associate on electromagnetic and piezoelectric MEMS devices at the University of Southern California's Department of Electrical Engineering. In January 2004, he joined the LCD Development Center of Samsung Electronics as a Senior Engineer, where

he is working on optical and thermal feedback control of TFT-LCDs using integrated sensors on glass. He was recognized with a Distinguished Paper Award at the 2005 SID International Symposium and has published over 20 technical papers.



Seunghwan Moon is Principal Engineer at Samsung Electronics's LCD Business. He received his B.S. and M.S. degrees in electrical engineering from Yonsei University in Seoul, Korea. He joined Samsung in 1990 and has been working on the design and analysis of LCD driving circuits. He has developed and standardized a new LCD driving technique which features very low power consumption. Currently, he is leading the Technology Development Group at Samsung's LCD

Development Center, where his activities include circuit integration with α -Si:H TFTs on LCD panels.



Brian H. Berkeley is Vice President for Advanced Technology within Samsung's LCD business unit. He received his B.S. degree in electrical engineering from M.I.T and his M.S. degree in electrical engineering from Carnegie-Mellon University. He worked at Apple Computer for 20 years, starting as a display engineer on the original Macintosh. He led hardware development on the first iMac computer and ran Apple's display and hardware I/O engineering. His display innovations include

the first use of in-line gun CRTs in a monitor application, putting color onto the Macintosh platform, development of the world's first high-volume LCD monitor, and the first implementation of wide-format notebook and desktop LCDs. He served as Program Chair of the SID Symposium in 2000 and as General Chair in 2002. He joined Samsung Electronics in November, 2003, and his research activity includes development of advanced liquid-crystal driving technologies.



Sang Soo Kim received his B.S. degree in physics from Seoul National University, Seoul Korea, in 1983, and his Ph.D. degree in physics from North Carolina State University, in 1990. He joined Samsung Electronics as a principal engineer in 1990, where he has been working on active-matrix liquid-crystal displays. He played a key role in establishing the firm's TFT-LCD R&D team and has developed a variety of TFT-LCD products that

have positioned Samsung Electronics as the world's leading TFT-LCD supplier. Among his pioneering R&D activities, he developed an 82-in.-diagonal full-color wide UXGA TFT-LCD, the world's largest single-glass direct-view TFT-LCD, in 2005. Currently, he is a Senior Vice President of Samsung's LCD Business, where he has responsibility for research and development of the TFT-LCD products. He has published over 40 papers in technical journals and has been awarded 35 U.S. patents on various flat-panel-display devices. In recognition of his technical accomplishments, he was awarded the title of Samsung Fellow in 2005.